Am J Transl Res 2021;13(11):12285-12301
www.ajtr.org /ISSN:1943-8141/AJTR0133968

Original Article

Long noncoding RNA KCNQ1 opposite strand/antisense transcript 1 promotes osteosarcoma progression through miR-154-3p/KLF12

Qibo Zhang[1], Huachang Jiang[2], Youming Jin[3], Ning Zhang[4], Zhihua Mu[4], Yan Guo[5], Haitao Li[6]

[1]Department of Ultrasound, Weihai Municipal Hospital, Cheeloo College of Medicine, Shandong University, Weihai 264200, Shandong Province, China; [2]Trauma Surgery Department, Dongying District People's Hospital, Dongying 257100, Shandong Province, China; [3]Department of Orthopaedics, Gaoqing People's Hospital, Zibo 256300, Shandong Province, China; [4]Department of Orthopaedics, Zhaoyuan People's Hospital, Yantai 265400, Shandong Province, China; [5]Palliative Medicine Center, Xinkun Hua Hospital, The First People's Hospital of Yunnan Province, Kunming 650100, Yunnan Province, China; [6]Department of Joint Surgery, Linyi People's Hospital, Linyi 276000, Shandong Province, China

Received April 6, 2021; Accepted September 23, 2021; Epub November 15, 2021; Published November 30, 2021

Abstract: Objective: Osteosarcoma (OS) is a common bone cancer that usually influences children. Metastasis and recurrence are the main reasons for the poor prognosis. In this study, we investigated the functions and mechanisms of KCNQ1 opposite strand/antisense transcript 1 (KCNQ1OT1) in OS. Methods: Cell viability and proliferation were detected using the CCK-8 assay and the 5-Ethynyl-2'-deoxyuridine (EdU) assay. Wound-healing assays, transwell assay and flow cytometry were used to identify cell migration, invasion, and apoptosis, respectively. The relationship among KCNQ1OT1, miR-154-3p, and KLF12 was verified by luciferase reporter assay and restricting protein immunoprecipitation (RIP) assay. Xenograft models were established to confirm the function of KCNQ1OT1 in vivo. Results: The expression of KCNQ1OT1 was higher in OS than in non-tumor tissues and cells. Knockdown of KCNQ1OT1 could reduce OS cell proliferation, migration, and invasion and promoted cell death. Mechanistically, KCNQ1OT1 contributed to OS formation by acting as a competitive endogenous RNA (ceRNA) and influencing miR-154-3p expression. Furthermore, we confirmed that miR-154-3p affected KLF12 expression through binding the 3'UTR region. Finally, rescue experiments determined that KCNQ1OT1 exerted major roles in OS through the miR-154-3p/KLF12 axis. Conclusion: In conclusion, our research explains the mechanism of KCNQ1OT1 in OS progression, which could serve as a new therapeutic target.

Keywords: Osteosarcoma, KCNQ1 opposite strand/antisense transcript 1, miR-154-3p, KLF12

Introduction

Osteosarcoma (OS) is a bone cancer that frequently happens in children and accounts for about 60% of all life-threatening bone tumors. In OS, primitive altered cells differentiate into osteoblasts and produce malignant osteoid tissue [1-3]. Currently, the main treatment of OS is surgical resection combined with radiotherapy and chemotherapy [4]. Patients with local OS have a 5-year survival rate of roughly 70%, while tumor metastasis or recurrence reduces the overall survival rate to less than 20% [5]. Hence, it is crucial to inhibit cancer cell metastasis in OS. Although previous research has reported some molecular targets contributing to OS tumorigenesis and development, the mechanism is uncertain [6, 7]. Therefore, further studies are needed on OS progression to develop a novel therapeutic method for OS.

In various diseases, lncRNAs dysregulation is associated with aberrant cell proliferation, apoptosis, migration and invasion, and even resistance [8-10]. In bladder cancer, for example, lncRNA GClnc1 levels are drastically increased, promoting cell proliferation, metastasis, and invasiveness through the LIN28B/let-7a/MYC pathway [11]. Besides, studies have found that lncRNA performs its function by sponging miR-

Table 1. Sequence of vectors used for transfection

	Sequence (5'-3')
sh-NC	TTCTCCGAACGTGTCACGT
sh-KCNQ1OT1	TTGCTGGTTACTGGCTTGAAA
miR-154-3p mimic	AAUCAUACACGGUUGACCUAUU
miR-154-3p inhibitor	GGUACUUGAAGAUAGGUUA
mimic NC	UUCUCCGAACGUGUCACGUTT
inhibitor NC	CAGUACUUUUGUGUAGUACAA
sh-KLF12	GGTTGAGTACCACAATTAAC

Note: NC: negative control; KCNQ1OT1: KCNQ1 opposite strand/antisense transcript 1.

NAs and affecting their target gene expression [12, 13]. LncRNA KCNQ1 opposite strand/antisense transcript 1 (lncRNA KCNQ1OT1) has been shown to participate in various diseases, including cancer. For instance, KCNQ1OT1 promotes cell expansion and metastasis through sponging miR-145-5p and up-regulating PCBP2 expression in malignant bladder cancer [14]. KCNQ1OT1 enhances the drug resistance in colon cancer and tongue cancer [15, 16]. However, the roles of KCNQ1OT1 in OS and its underlying mechanism have not been fully elucidated.

In this study, we investigated the roles and the mechanism of KCNQ1OT1 in OS. These results may provide new targets for OS therapy.

Materials and methods

Clinical sample

Clinical tissue samples, including OS tumor tissues and para-cancerous tissues, were collected from pathologically confirmed patients. The tissue samples were promptly stored in liquid nitrogen or a -80°C refrigerator for future investigation. After being informed, all patients in this trial signed a consent form. The study was approved by the hospital's Ethics Committee (LYRY-2019-0058).

Cell culture

OS cell lines U2OS, 143B, 6T-CEM, HOS, and osteoblast cell line hFOB1.19 were purchased from Cell Resource Center of Shanghai Academy of Science. U2OS cells were cultivated in McCoy's 5A medium, HOS cells in MEM, and 143B cells in Dulbecco's Modified Eagle medium (DMEM), 6T-CEM cells in Roswell Park Memorial Institute (RPMI) 1640 medium, hFOB1.19 cells in DMEM/F12 medium. All the culture medium was purchased from Thermo Fisher, and were enhanced with 10% FBS (fetal bovine serum) and 1% penicillin-streptomycin (MP Biomedicals, CA, USA). The cells were passaged twice or three times a week in incubators that maintained 5% CO_2 and 37°C.

Cell transfection

When the cells reached 80% confluence, the lncRNA KCNQ1OT1 shRNA lentiviruses (GenePharma, Shanghai, China) were transfected into U2OS and HOS to obtain stable KCNQ1OT1 knockdown cells. Control shRNA lentiviruses were used as controls. U2OS and HOS were transfected with negative control (NC) mimics, miR-154-3p inhibitor, miR-154-3p mimics, and NC inhibitor (GenePharma, Shanghai, China) to detect the effects of miR-154-3p in OS cells. MiR-154-3p inhibitors and KLF12 shRNA (GenePharma, Shanghai, China) were simultaneously transfected into U2OS/sh-KCNQ1OT1 and HOS/sh-KCNQ1OT1 to study downstream effectors of KCNQ1OT1. The sequences of vectors used for transfection are listed in **Table 1**.

Real-time quantitative polymerase chain reaction (RT-qPCR)

Total RNA was extracted from clinical tissues and cells using the TRIzol reagent (ThermoScientific, MA, USA). The PrimeScript RT reagent Kit with Eraser was used to reverse-transcribe RNA to cDNA (Takara, Japan). Subsequently, RT-qPCR was performed on an Applied Biosystems 7300 sequence detection system (Applied Biosystems, USA) using a Vazyme SYBR green PCR kit (Nanjing, China). To standardize the general expression of miRNAs and genes, U6 and GAPDH were utilized. The reaction procedures of RT-qPCR were according to the instructions. The RT-qPCR primers are shown in **Table 2**.

Cell viability assay

CCK-8 assay was used to determine cell viability. First, cells were plated in 96-well plates at a density of 10^3 cells/well. Then the cells were cultured with 10 μL CCK8 reagent (Dojindo, Kumamoto, Japan) for two hours. Finally, the optical density at 450 nm was measured by uti-

Table 2. Primers used for RT-qPCR

	Forward (5'-3')	Reverse (5'-3')
KCNQ1OT1	ACTCACTCACTCACTCACT	CTGGCTCCTTCTATCACATT
KLF12	CGGCAGTCAGAGTCAAAACAG	CGGCTTCCATATCGGGATAGT
SP3	CCGCTACCTGCAGCAAGAT	AAGCCAAATCACCTGTCGCT
DYRK1A	GCTGGAACCGCGAGCC	GCGGCAAAACTATAACACGGG
PCGF3	CAGGCGTCGTGCTCAGAAAA	ATGCATACTGAGGACACGGG
SREK1	TTCGGTTTGGGCTTAGGCTT	GCAAGAGGTGCGTTGTCCG
PDE10A	CTTCGGCTCCGACATGGAAG	TCATCTGTCAAACTGGGGCTC
TREM178B	TGCTCTTCCTCATGGGAGATTC	CCACTTAGAGCGTGCCATCT
GAPDH	TCTCTGCTCCTCCTGTTC	GTTGACTCCGACCTTCAC
miR-154-3p	AAUCAUACACGGUUGACCUAUU	AATAGGTCAACCGTGTATGATT
miR-183-5p	UAUGGCACUGGUAGAAUUCACU	AGTGAATTCTACCAGTGCCATA
miR-506-3p	UAAGGCACCCUUCUGAGUAGA	TCTACTCAGAAGGGTGCCTTA
miR-124-3p	UAAGGCACGCGGUGAAUGCCAA	TTGGCATTCACCGCGTGCCTTA
miR-487-3p	AAUCAUACAGGGACAUCCAGUU	AACTGGATGTCCCTGTATGATT
miR-487a-3p	AAUCAUACAGGGACAUCCAGUU	AACTGGATGTCCCTGTATGATT
miR-103a-3p	AGCAGCAUUGUACAGGGCUAUGA	TCATAGCCCTGTACAATGCTGCT
miR-301a-3p	CAGUGCAAUAGUAUUGUCAAAGC	GCTTTGACAATACTATTGCACTG
miR-301b-3p	CAGUGCAAUGAUAUUGUCAAAGC	GCTTTGACAATATCATTGCACTG
miR-454-3p	UAGUGCAAUAUUGCUUAUAGGGU	ACCCTATAAGCAATATTGCACTA
U6	GCTTCGGCAGCACATATACT	AACGCTTCACGAATTTGCGT

Note: KCNQ1OT1: KCNQ1 opposite strand/antisense transcript 1; RT-qPCR: Real-time quantitative polymerase chain reaction.

lizing a Bio-EL340 automatic microplate reader (Tek Instruments, Hopkinton, USA).

EdU assay

EdU assays were carried out using RiboBio's Cell-Light EdU image detection kit. Cells were plated into 96-well plates at a density of 4×10^3-1×10^5/well and cultured with 100 μL EdU medium for two hours. Then the medium was removed, and cells were fixed in 4% formaldehyde for 15 minutes before being treated with 0.5% Triton X-100 for 20 minutes. Finally, the Apollo reaction cocktail was added to the cells. The results were visualized under the fluorescence microscope (Nikon, Tokyo, Japan).

Cell apoptosis analysis in cells and tissues

Flow cytometry was used to identify cell apoptosis. Cells were treated with Annexin V and PI for 15 minutes at room temperature. FACS was used to examine the labeled cells (Leica, Wetzlar, Germany). Each experiment was carried out in triplicate.

Cell apoptosis in tissues was detected using Tunnel labeling assay. Paraffin was used to fix and embed the tissues. The Roche In-Situ Cell Death Detection Kit was used to stain sections according to the manufacturer's instructions (Basel, Switzerland). After staining, sections were examined under the microscope (Nikon, Tokyo, Japan).

Wound-healing assay

The cells were cultivated after being seeded onto 6-well plates with a complete medium. Then we used a 200 μL pipette tip to scratch cells that were in a single layer. Detached cells were removed by using serum-free medium washing twice. The cells were also grown for additional 24 hours, and the injured areas were inspected and imaged using inverted microscopy (Leica, Wetzlar, Germany). Each experiment was carried out in triplicate.

Transwell invasion assay

The cells were seeded into the top compartment. After incubation for 24 h or 48 h, the cells in the bottom compartment were quantified by using crystal violet. Bio-Coat Matrigel invasion chambers were used in the invasion assay (Merk Millipore, Darmstadt, Germany). The cells were plated on Matrigel-coated filters, and a chemoattractant of FBS (5%) was applied to the lower chambers. After that, the chambers were cleaned with PBS and incubated for 24 hours. Crystal violet (0.1%) was used to fix and stain the invaded cells in lower chamber. Each experiment was carried out in triplicate.

Western blot analysis

U2OS and HOS cells that transfected with sh-NC, sh-KCNQ1OT1, NC mimic, and miR-154-3p mimics were collected. To lyse the cell and extract the protein, we employed RIPA lysis buffer with protease inhibitors. The entire protein extraction procedure was performed on ice. The extracted protein was quantified using a

BCA protein assay kit (Thermo-Scientific, MA, USA). 20 μg of protein samples were separated by 10% SDS-PAGE before being transferred to a polyvinylidene difluoride membrane (Millipore, Bedford, USA). Layers were then blocked for 2 hours at room temperature with 5% nonfat milk containing 0.1% PBST to restrain vague restricting. The membranes were then incubated with the primary antibody overnight at 4°C. Later, the blot was incubated with matching secondary antibodies for 2 hours at room temperature. An enhanced chemiluminescence kit was used (Vazyme, Nanjing, China) to image the blots. β-actin was used as an internal control. The protein bands were measured using the Image J software.

The primary antibody included PCNA (ab29, 1:1000), Ki67 (ab15580, 1:1000), Bax (ab32503, 1:1000), Bcl-2 (ab32124, 1:1000), Cleaved-caspase-3 (ab2302, 1:500), Cleaved-caspase-9 (ab2324, 1:200), MMP-2 (ab92536, 1:1000), MMP-9 (ab76003, 1:1000), KLF12 (ab221602, 1:2000), β-actin (ab6276, 1:5000) and Cox-2 (Cell Signaling Technology, 4842, 1:200). The secondary antibody was goat anti-rabbit HRP antibody (ab6721, 1:5000).

Luciferase reporter assay

The anticipated miR-154-3p binding sites were amplified and inserted into the luciferase reporting plasmids (General Biol, Anhui, China). The sequences of KCNQ1OT1 that interacted with miR-154-3p were modified, and the mutant sequences were put into an identical luciferase reporter plasmid to test binding specificity. For the luciferase reporter test, U2OS and HOS cells were cultured on 24-well plates. Each well was transfected with 0.5 μg of luciferase reporter plasmid. Lipofectamine 2000 (Thermo-Scientific, Massachusetts, USA) was used to deliver 100 nM miR-154-3p mimic or control mimic. A luciferase assay kit was used to analyze luciferase signals 48 hours after transfection, following the manufacturer's procedure (Promega Corporation, Wisconsin, USA).

RNA-binding protein immunoprecipitation (RIP)

Millipore's Magna RNA immunoprecipitation kit (Bedford, USA) was utilized in the RIP investigation. U2OS and HOS cells were lysed using RIP buffer. After that, Anti-Argonaute2 or immunoglobulin G-coated magnetic beads were used to incubate the cell lysis (Abcam, USA). After purifying RNAs in magnetic beads, RT-qPCR was used to detect enrichment of KCNQ1OT1 and miR-154-3p.

Mouse xenograft model

Nude mice (4-6 weeks, 18-22 g) were obtained from GemPharmatech (Nanjing, China). U2OS cells stably expressing sh-KCNQ1OT1 and sh-NC were injected subcutaneously into the left flank of mice. We measured the tumor volume every five days. After four weeks, mice were euthanized. The tumor size was measured every week by using calipers [(length × width^2)/2]. Tumor weight was assessed and recorded after mice were euthanized with 1% pentobarbital sodium (90 mg/kg, Dainippon Sumitomo Pharma). The tumor was maintained in the properconditions for subsequent investigation.

Hematoxylin and Eosin staining

The tumor tissues of nude mice were excised and fixed in 4% paraformaldehyde for 24 hours. Next, tumor tissues were fixed in paraffin and cut into 4 μm slices. The Hematoxylin and Eosin procedure was used to stain tissue slices. Image J software (version k 1.45) was used to determine the quantification of the staining (NIH, Bethesda, MD, USA).

Immunohistochemistry (IHC) staining

The tissue sections were deparaffinized and rehydrated using ethanol gradients after being deparaffinized with xylene. Then, tissue pieces were treated in citrate buffer to extract antigen. The sections were blocked with regular goat serum and then incubated with Ki67 (1:500, Abcam, Cat: ab15580, USA) and goat anti-rabbit HRP antibody (1:5000, Abcam, Cat: ab6721, USA) for the immunostaining. Finally, samples were stained with diaminobenzidine (DAB, Sigma-Aldrich, USA). The sections were dehydrated, mounted, and photographed using an optical microscope (Nikon, Tokyo, Japan), and then analyzed by Image Pro Plus 6.0 (BIO-IMAG, USA).

Statistical analysis

The data were represented by the mean ± standard deviation ($\bar{x}$±sd) of three independent

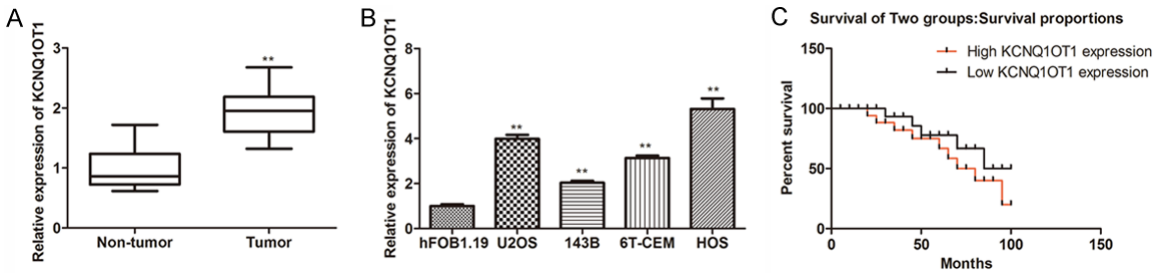

Figure 1. The LncRNA KCNQ1OT1 expression in OS tissues and cells. A: The expression of lncRNA KCNQ1OT1 in OS and non-tumor tissues was detected by RT-qPCR; B: RT-qPCR detected the expression of KCNQ1OT1 in normal osteoblast cells hFOB1.19 and OS cell line U2OS, 143B, 6T-CEM, HOS; C: The overall survival rates of OS patients were compared in KCNQ1OT1 high expression and low expression groups. $^{**}P<0.01$, * as the difference of OS group and normal group. Error bars were represented the mean ± standard deviation ($\bar{x}$ ± sd) of triplicate experiments. OS: Osteosarcoma; lncRNA: Long non-coding RNA; KCNQ1OT1: LncRNA KCNQ1 opposite strand/antisense transcript 1; RT-qPCR: Real-time quantitative polymerase chain reaction.

experiments. The mean difference between groups was determined using an unpaired Student t-test. For comparison among multiple groups, a one-way ANOVA followed with Bonferroni post hoc test was conducted. Statistical analysis was performed using SPSS 13.0 software (SPSS, Chicago, IL, USA) and GraphPad Prism7 program (GraphPad Inc., San Diego, CA, USA). *P*-value of 0.05 was used as the cutoff for statistical significance.

Results

KCNQ1OT1 was up-regulated in OS tissues and cell lines

We collected 16 matched OS tissues and non-tumor tissues from the confirmed patient to examine the expression of lncRNA KCNQ1OT1 in the development of OS. KCNQ1OT1 expression was elevated in OS tissues and cell lines (U2OS, 143B, 6T-CEM, HOS) (**Figure 1A**, **1B**). Furthermore, Kaplan-Meier survival analysis demonstrated that increased KCNQ1OT1 expression in OS patients was associated with a lower overall survival rate (**Figure 1C**). These findings indicate that KCNQ1OT1 plays a role in the development of OS.

Knocking down KCNQ1OT1 inhibited proliferation and induced apoptosis of OS cells

To evaluate the regulatory role of KCNQ1OT1 in the OS process, we knocked down KCNQ1OT1 by transfecting KCNQ1OT1 siRNA into U2OS and HOS cells (**Figure 2A**). The KCNQ1OT1 knockdown suppressed cell proliferation (**Figure 2B**, **2C**) and increased cell apoptosis (**Figure 2E**) of U2OS and HOS cells. The expressions of proliferation-related genes, PCNA and Ki67, were downregulated in KCNQ1OT1 knockdown cells (**Figure 2D**). KCNQ1OT1 knockdown promoted the protein expression of Bax, cleaved caspase 3, and cleaved caspase 9 while inhibiting the expression of Bcl-2 in U2OS and HOS cells (**Figure 2F**). These findings indicate that KCNQ1OT1 knockdown inhibited OS cell proliferation and increased cell apoptosis.

KCNQ1OT1 depletion inhibited migration and invasion of OS cells

The function of NQ1OT1 knockdown in OS cells was further studied. Wound healing assays, transwell invasion assays, and western blotting were adopted to investigate the role of KCNQ1OT1 in migration and invasion. As illustrated in **Figure 3A**, **3B**, downregulation of KCNQ1OT1 inhibited migration and invasion of U2OS and HOS cells. In addition, the western blot results also showed that knockdown of KCNQ1OT1 decreased cell migration and invasion-related genes, Cox-2, MMP-2 and MMP-9, in U2OS and HOS cells (**Figure 3C**).

KCNQ1OT1 was predicted to bind with miR-154-3p and suppressed its expression

Increasing evidence suggests that KCNQ1OT1 exerts its roles through sponging miRNA. Using the ENCORI database, we found 508 miRNAs that have the potential to interact with KCNQ1OT1, among which miR-154-3p expression was shown to be significantly decreased in OS cells (**Figure 4A**). LncRNA KCNQ1OT1 and miR-154-3p putative binding site are displayed in

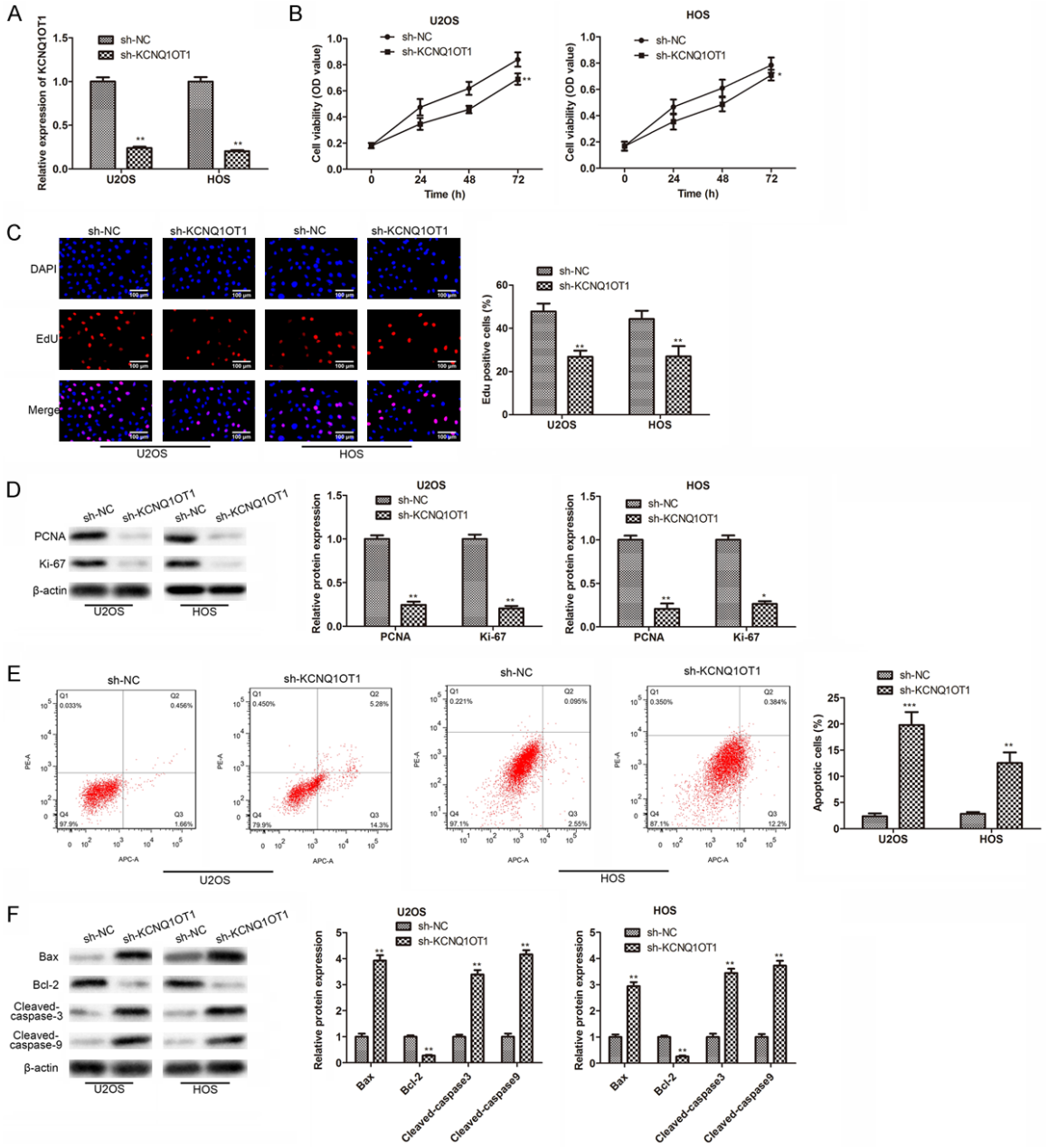

Figure 2. Knockdown of KCNQ1OT1 inhibits OS cell proliferation and promotes cell apoptosis. A: The efficiency of KCNQ1OT1 knockdown was detected by RT-qPCR; B: The effect of KCNQ1OT1 knockdown on cell viability was detected by CCK8 assay; C: The effect of KCNQ1OT1 knockdown on cell proliferation was detected by EdU assay and statistics EdU-positive cells rate (400×); D: Western blot was used to detect the proliferation-related genes expression; E: Flow cytometry detected cell apoptosis difference in KCNQ1OT1 downregulated OS cells; F: The protein levels of apoptosis-related genes were detected by western blot. ***P<0.001, **P<0.01, *P<0.05. The difference is compared with cells that transfected sh-NC. Error bars were represented the mean ± standard deviation ($\bar{x}$ ± sd) of triplicate experiments.OS: Osteosarcoma; KCNQ1OT1: KCNQ1 opposite strand/antisense transcript 1; NC: negative control; RT-qPCR: Real-time quantitative polymerase chain reaction; EdU 5-Ethynyl-2'-deoxyuridine.

Figure 4B. To confirm the interaction between miR-154-3p and KCNQ1OT1, we co-transfected Wt-KCNQ1OT1 vectors or Mut-KCNQ1OT1 vectors with miR-154-3p mimics. Cells co-transfected with miR-154-3p mimics and WT-KCNQ1OT1 had significantly decreased luciferase activity compared to cells co-transfected with miR-154-3p mimics and Mut-KCNQ1OT1

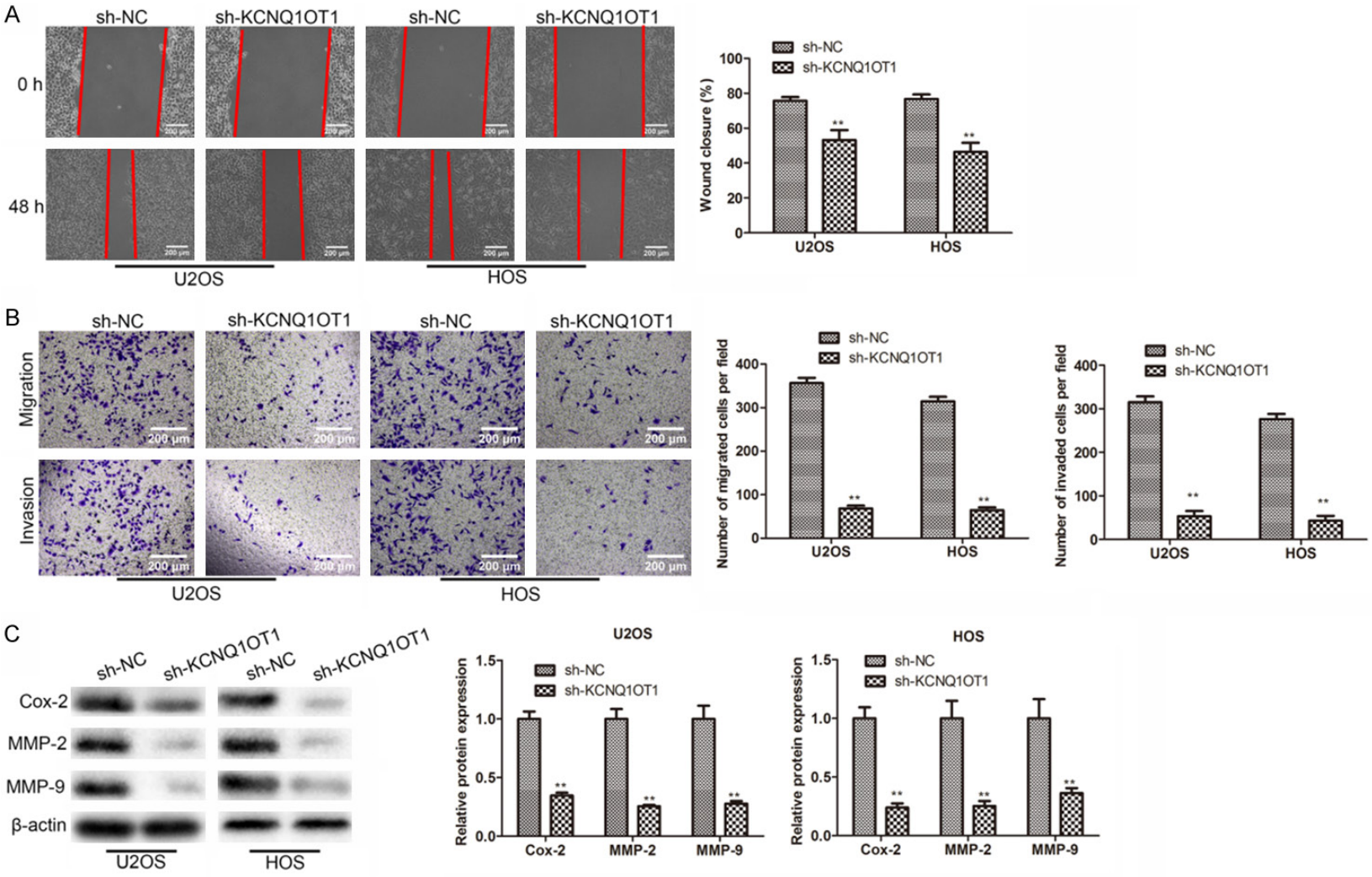

Figure 3. Knockdown of KCNQ1OT1 inhibits OS cell migration and invasion; A: The effect of KCNQ1OT1 knockdown on cell migration was detected by wound-healing assay (100×); B: Transwell assay was used to detect cell migration and invasion in OS cells that transfected sh-KCNQ1OT1 or sh-NC (100×); C: Western blot measured protein levels of related cell migration and cell invasion genes. $^{**}P<0.01$, * as the difference of sh-KCNQ1OT1 group cells compared with sh-NC group cells. Error bars were represented the mean ± standard deviation ($\bar{x}$ ± sd). Results represent the average of three independent experiments. OS: Osteosarcoma; KCNQ1OT1: KCNQ1 opposite strand/antisense transcript 1; NC: negative control.

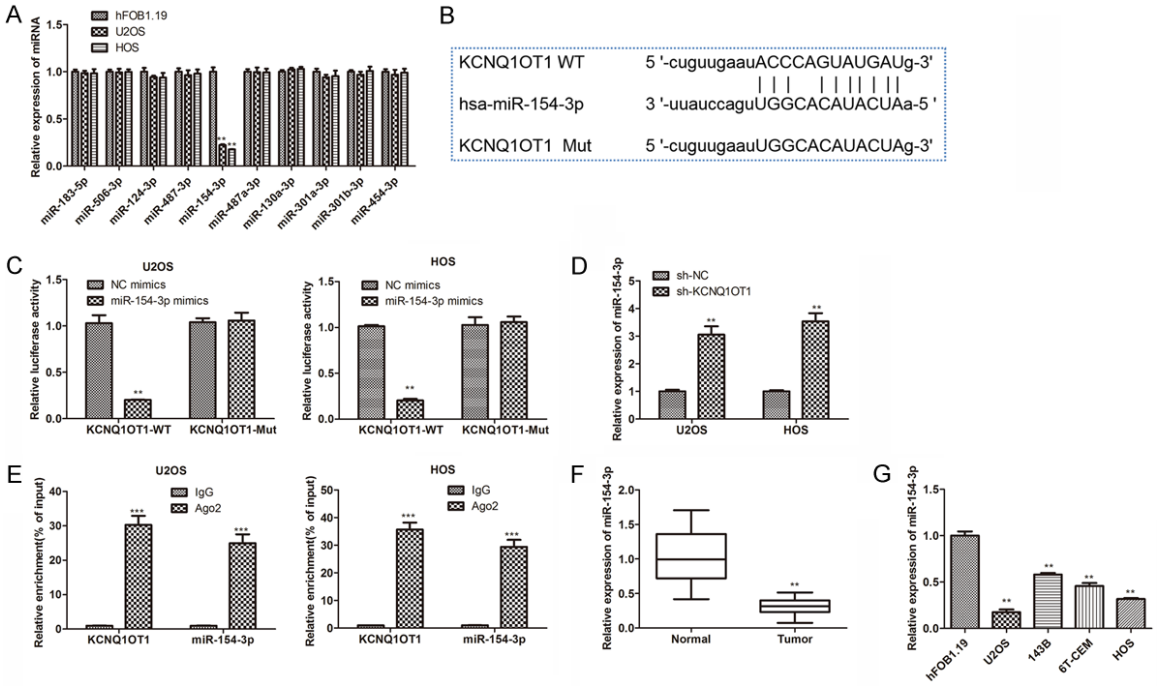

Figure 4. KCNQ1OT1 binds to miR-154-3p and inhibits its expression. A: RT-qPCR detected miRNAs expression in normal osteoblast cells and OS cells; B: The putative miR-154-3p binding sites wild-type and mutant in KCNQ1OT1; C: The relative luciferase activity of cells co-transfected with constructed luciferase reporters (Wt-KCNQ1OT1 and Mut- KCNQ1OT1), pRL-TK vectors and miR-154-3p mimics or negative control; D: The expression of miR-154-3p was detected by RT-qPCR in U2OS and HOS cells transfected sh-KCNQ1OT1; E: Anti-AGO2 RIP was performed in U2OS and HOS cells, followed by RT-qPCR to detect KCNQ1OT1 and miR-154-3p expression; F: The expression of miR-154-3p was detected by RT-qPCR in OS non-tumor and tumor tissues; G: The expression of miR-154-3p was detected by RT-qPCR in normal osteoblast cells and OS cells. Compared with the control group, ***P<0.001, **P<0.01. Error bars were represented the mean ± standard deviation ($\bar{x}$ ± sd) of triplicate experiments. OS: Osteosarcoma; KCNQ1OT1: KCNQ1 opposite strand/antisense transcript 1; NC: negative control; RT-qPCR: Real-time quantitative polymerase chain reaction.

cells (**Figure 4C**). Additionally, miR-154-3p expression was dramatically increased in KCNQ1OT1 knockdown OS cells (**Figure 4D**). The enrichment of KCNQ1OT1 and miR-154-3p in the Ago2 RIP group was higher than in the IgG group (**Figure 4E**), indicating MiR-154-3p interacted with KCNQ1OT1. Following that, we determined the expression of miR-154-3p in OS tissues and cells. MiR-154-3p expression was observed to be down-regulated in OS tissues and cells when compared to non-tumor tissues and osteoblast cells (**Figure 4F**, **4G**). These findings revealed that miR-154-3p inhibited KCNQ1OT1 in OS.

Overexpression of MiR-154-3p decreased growth, migration, and invasion, and promoted apoptosis of OS cells

miR-154-3p mimics was transfected into U2OS and HOS cells to investigate the regulatory implications of miR-154-3p in the OS process. First, the miR-154-3p overexpression efficiency was determined using RT-qPCR (**Figure 5A**). Next, CCK-8 and EdU assay were used to detect cell viability, and the results showed that miR-154-3p overexpression inhibited cell growth (**Figure 5B**, **5C**) but promoted cell apoptosis (**Figure 5D**) in U2OS and HOS cells. Next, the effects of miR-154-3p overexpression on cell migration and invasion were studied. In U2OS and HOS cells, miR-154-3p mimics inhibited cell migration and invasion, as shown by Transwell assay (**Figure 5E**). These data suggest that miR-154-3p acts as a tumor suppressor gene in OS cells, preventing cell proliferation, migration, and invasion while boosting cell death.

KLF12 was predicted to be a miR-154-3p target gene

KCNQ1OT1 could sponge miR-154-3p based on the preceding findings. However, the downstream gene of miR-154-3p still needs further

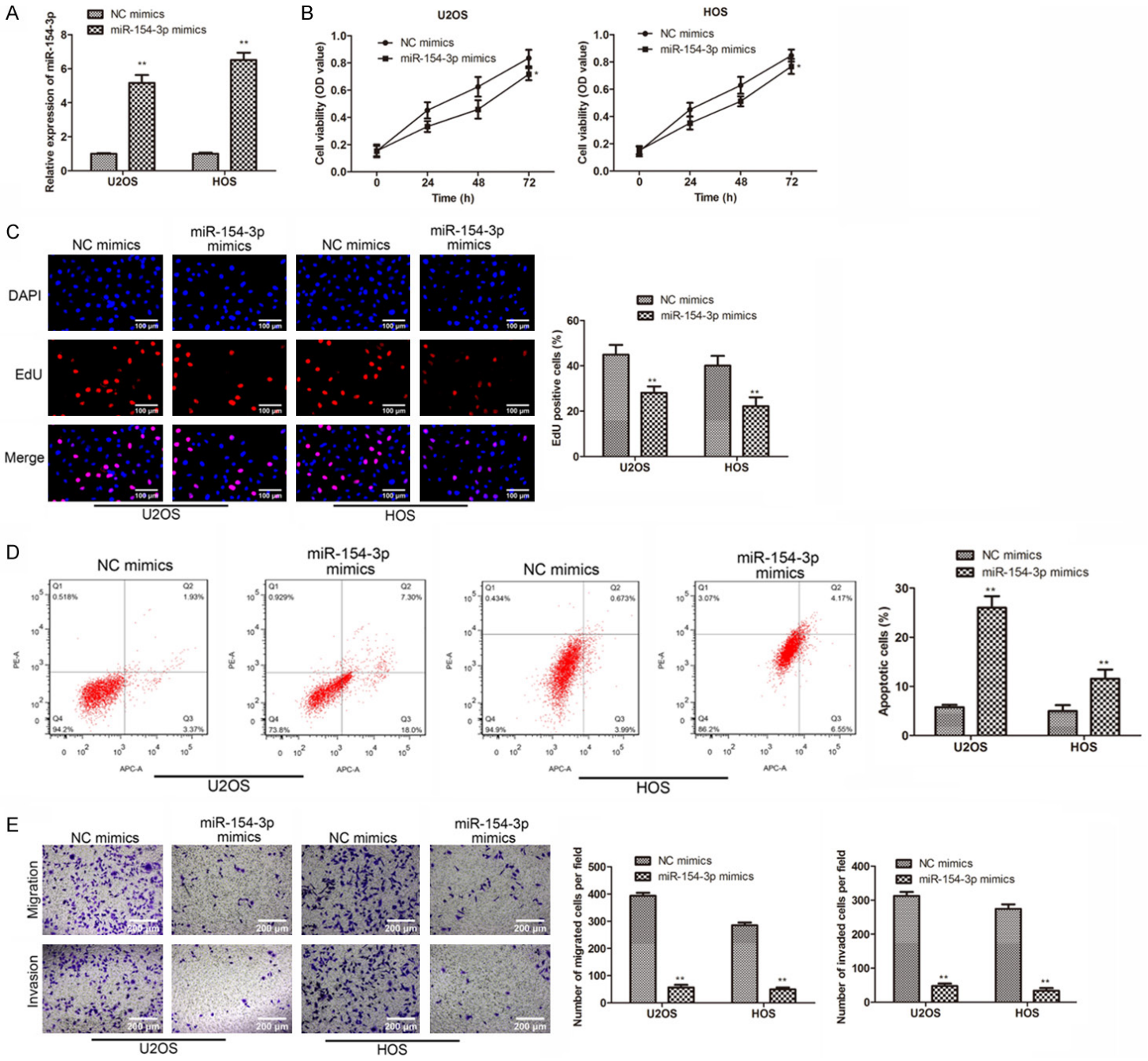
A
NC mimics
miR-154-3p mimics
Relative expression of miR-154-3p
U2OS
HOS
B
U2OS
HOS
NC mimics
miR-154-3p mimics
Cell viability (OD value)
Time (h)
C
NC mimics
miR-154-3p mimics
DAPI
EdU
Merge
U2OS
HOS
EdU positive cells (%)
D
NC mimics
miR-154-3p mimics
Apoptotic cells (%)
E
Migration
Invasion
Number of migrated cells per field
Number of invaded cells per field

Figure 5. Overexpression of miR-154-3p inhibits OS cell proliferation, migration, invasion and promotes cell apoptosis. U2OS and HOS cells transfected miR-154-3p mimics and NC mimics respectively. A: Efficiency of miR-154-3p overexpression was detected by RT-qPCR; B: The effect of miR-154-3p overexpression on cell viability was detected by CCK8 assay; C: EdU assay detected the effect of miR-154-3p overexpression on cell proliferation (400×); D: Flow cytometry detected cell apoptosis difference in transfected miR-154-3p mimics and NC mimics OS cells; E: Transwell assay was used to detected cell migration and invasion in transfected miR-154-3p mimics and NC mimics OS cells (100×). Compared with the NC mimics group, $^{**}P<0.01$, $^{*}P<0.05$. Error bars were represented the mean ± standard deviation ($\bar{x}$ ± sd). Every experiment three independent repetitions. OS: Osteosarcoma; NC: negative control; RT-qPCR: Real-time quantitative polymerase chain reaction.

research. Bioinformatics analysis using ENCORI, miRwalk, and Targetscan suggested 7 possible downstream genes of miR-154-3p in the three predictive results. Then we discovered that only KLF12 expression was significantly higher in U2OS and HOS cells when compared to other anticipated genes (**Figure 6A**). The predicted binding site between KLF12 and miR-154-3p is displayed in **Figure 6B**. MiR-154-3p mimics significantly reduced luciferase activity of U2OS and HOS cells transfected with WT-KLF12 compared with the cells transfected with Mut-KLF12 (**Figure 6C**). Then, we detected KLF12 expression in U2OS and HOS cells overexpressing miR-154-3p. RT-qPCR and western blot results showed that KLF12 expression was decreased in miR-154-3p mimic-transfected OS cells compared to NC mimic-transfected OS cells (**Figure 6D**, **6E**). The expression of KLF12 in OS tissues and cells was then detected using RT-qPCR, and the result showed that compared to non-tumor tissues and osteoblast cells, KLF12 expression was up-regulated in OS tissues and cells (**Figure 6F**, **6G**). These findings indicate that KLF12 is a target gene of miR-154-3p, and miR-154-3p inhibits KLF12 expression in OS.

KCNQ1OT1 promoted cell progression by the miR-154-3p/KFL12 pathway in OS cells

To further verify the effect of KCNQ1OT1 on cell progression through miR-154-3p/KLF12 in OS, we transfected miR-154-3p inhibitor and sh-KLF12 in U2OS/sh-KCNQ1OT1 and HOS/sh-KCNQ1OT1 cells, separately or simultaneously. RT-qPCR was used to determine the knockdown efficiency of MiR-154-3p inhibitor and sh-KLF12, and the results are displayed in **Figure 7A**. Cell viability results suggested that knockdown of miR-154-3p retarded the inhibition of cell proliferation by KCNQ1OT1 knockdown. Simultaneous knockdown of MiR-154-3p and KLF12 reversed the cell proliferation induced by miR-154-3p knockdown in U2OS/sh-KCNQ1OT1 and HOS/sh-KCNQ1OT1 cells (**Figure 7B**, **7C**). Coincident with these results, flow cytometry assay showed that downregulation of miR-154-3p decreased the cell apoptosis, which was reversed by KLF12 knockdown in OS/sh-KCNQ1OT1 cells (**Figure 7D**). Knocking down miR-154-3p boosted cell migration and invasion in OS/sh-KCNQ1OT1 cells, and this was also reversed by KLF12 knockdown. (**Figure 7E**). The results showed that KCNQ1OT1 boosted cell proliferation, migration, and invasion in OS cells while suppressing cell death through the miR-154-3p/KFL12 pathway.

KCNQ1OT1 knockdown inhibited OS xenograft growth

To demonstrate the role of KCNQ1OT1 in OS carcinogenesis, we constructed a xenograft model by injecting sh-KCNQ1OT1 and sh-NC transfected OS cells into nude mice individually. Tumor growth was inhibited in the mice of the sh-KCNQ1OT1 group when compared to the sh-NC group (**Figure 8A**). Similarly, in the sh-KCNQ1OT1 group, tumor volume and weight were reduced (**Figure 8B**, **8C**). The H&E analysis suggested that inhibition of KCNQ1OT1 expression reduced the cell density and blurred cell borders of tumors. Meanwhile, in tumor tissues of sh-KCNQ1OT1 group, Ki67 expression, a proliferation marker, was downregulated compared to the sh-NC group. Furthermore, as shown in the tunnel staining result, the proportion of apoptotic cells in tumor tissues from the sh-KCNQ1OT1 group was higher than that in the control group (**Figure 8D**). Knocking down KCNQ1OT1 enhanced miR-154-3p expression while decreased KLF12 expression (**Figure 8E**). In conclusion, knocking down KCNQ1OT1 decreases OS xenograft growth *in vivo*.

Discussion

Abnormal lncRNA expression has been associated with cell proliferation, migration, invasion,

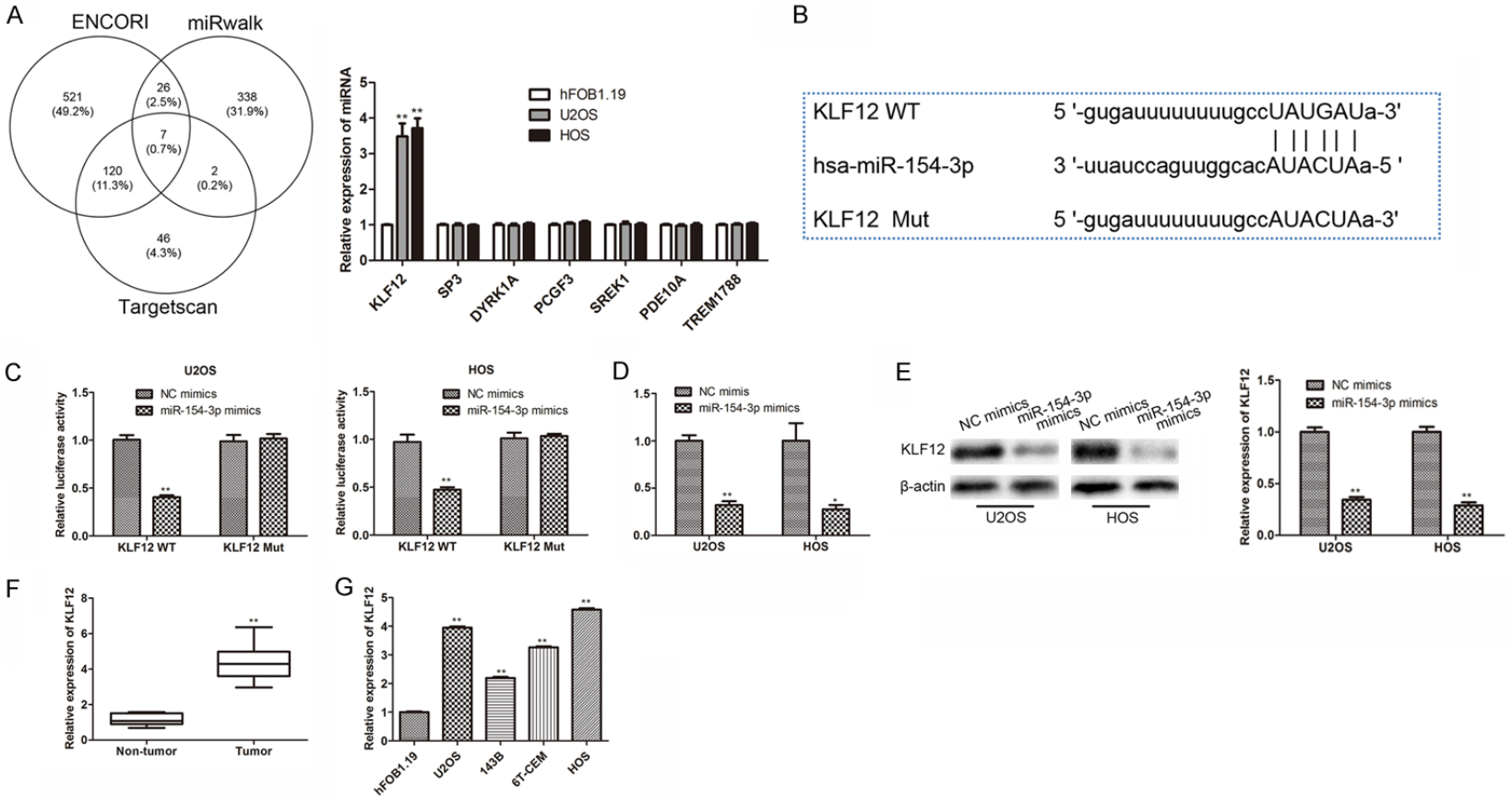

Figure 6. KLF12 is a direct target gene of miR-154-3p. A: Prediction target gene of miR-154-3p through ENCORI, TargetScan and miRWalk database, following RT-qPCR detected these target gene expressions in normal osteoblast cells and OS cells; B: The putative target sequence of miR-154-3p in KLF12 3'UTR and mutated sequence; C: Luciferase assays in U2OS and HOS cells transfected with wild type or mutant KLF12 and miR-154-3p mimics or NC mimics; D: RT-qPCR detected KLF12 expression in transfected miR-154-3p mimics OS cells; E: KLF12 expression in protein levels was detected by western blot in transfected miR-154-3p mimics OS cells; F: The expression of KLF12 was detected by RT-qPCR in OS non-tumor and tumor tissues; G: The expression of KLF12 was detected by RT-qPCR in normal osteoblast cells and OS cells. Compared with the control group, $^{**}P<0.01$, $^{*}P<0.05$. Error bars were represented the mean ± standard deviation ($\bar{x}$ ± sd) of triplicate experiments. OS: Osteosarcoma; NC: negative control; RT-qPCR: Real-time quantitative polymerase chain reaction.

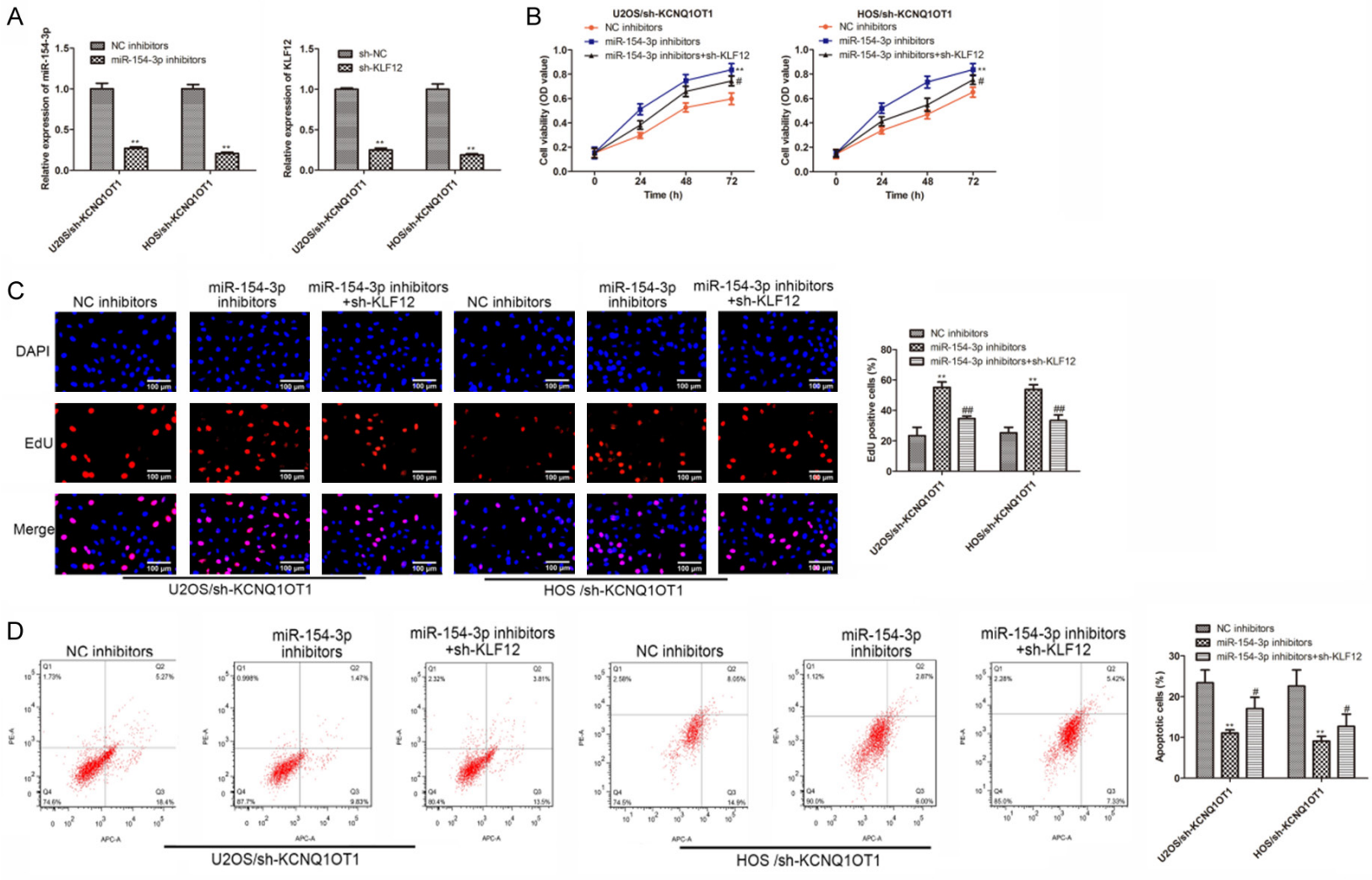
A
Relative expression of miR-154-3p
NC inhibitors
miR-154-3p inhibitors
U2OS/sh-KCNQ1OT1
HOS/sh-KCNQ1OT1
Relative expression of KLF12
sh-NC
sh-KLF12
B
U2OS/sh-KCNQ1OT1
HOS/sh-KCNQ1OT1
NC inhibitors
miR-154-3p inhibitors
miR-154-3p inhibitors+sh-KLF12
Cell viability (OD value)
Time (h)
C
NC inhibitors
miR-154-3p inhibitors
miR-154-3p inhibitors +sh-KLF12
DAPI
EdU
Merge
U2OS/sh-KCNQ1OT1
HOS /sh-KCNQ1OT1
EdU positive cells (%)
D
Apoptotic cells (%)

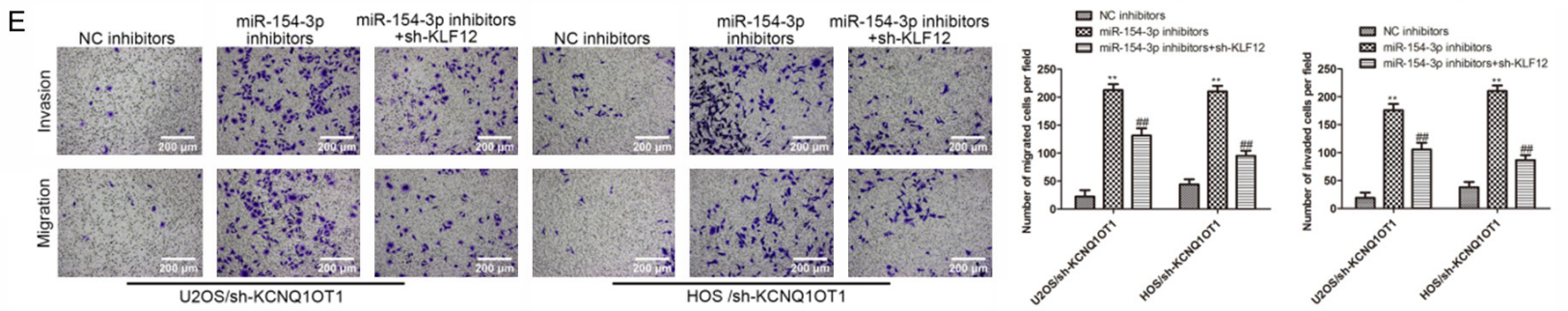

Figure 7. KCNQ1OT1 promotes the progression of osteosarcoma via regulating miR-154-3p/KLF12 axis. Knockdown KCNQ1OT1 stable strain was constructed in U2OS and HOS cells. U2OS/sh-KCNQ1OT1 and HOS/sh-KCNQ1OT1 transfected NC inhibitor, miR-154-3p inhibitor, sh-NC and sh-KLF12 respectively. U2OS/sh-KCNQ1OT1 and HOS/sh-KCNQ1OT1 transfected miR-154-3p inhibitor and sh-KLF12 simultaneously; A: The efficiency of knockdown miR-154-3p and KLF12 was detected by RT-qPCR; B: CCK8 assay detected the cell viability in knockdown miR-154-3p group cells solely and both knockdown miR-154-3p and KLF12 group cells; C: Cell proliferation was detected by EdU assay in transfected miR-154-3p inhibitor cells and simultaneously transfected miR-154-3p inhibitor and sh-KLF12 cells (100×); D: Cell apoptosis was detected by flow cytometry in the cells that described above; E: Transwell assay was used to measured cell migration and invasion ability (100×). Compared with NC inhibitor group or sh-NC group, $^{**}P<0.01$; Compared with miR-154-3p inhibitors group, $^{\#\#}P<0.01$, $^{\#}P<0.05$. Results represent the average of three independent experiments, error bars were represented the mean ± standard deviation ($\bar{x}$ ± sd). OS: Osteosarcoma; KCNQ1OT1: KCNQ1 opposite strand/antisense transcript 1; NC: negative control; RT-qPCR: Real-time quantitative polymerase chain reaction; EdU 5-Ethynyl-2'-deoxyuridine.

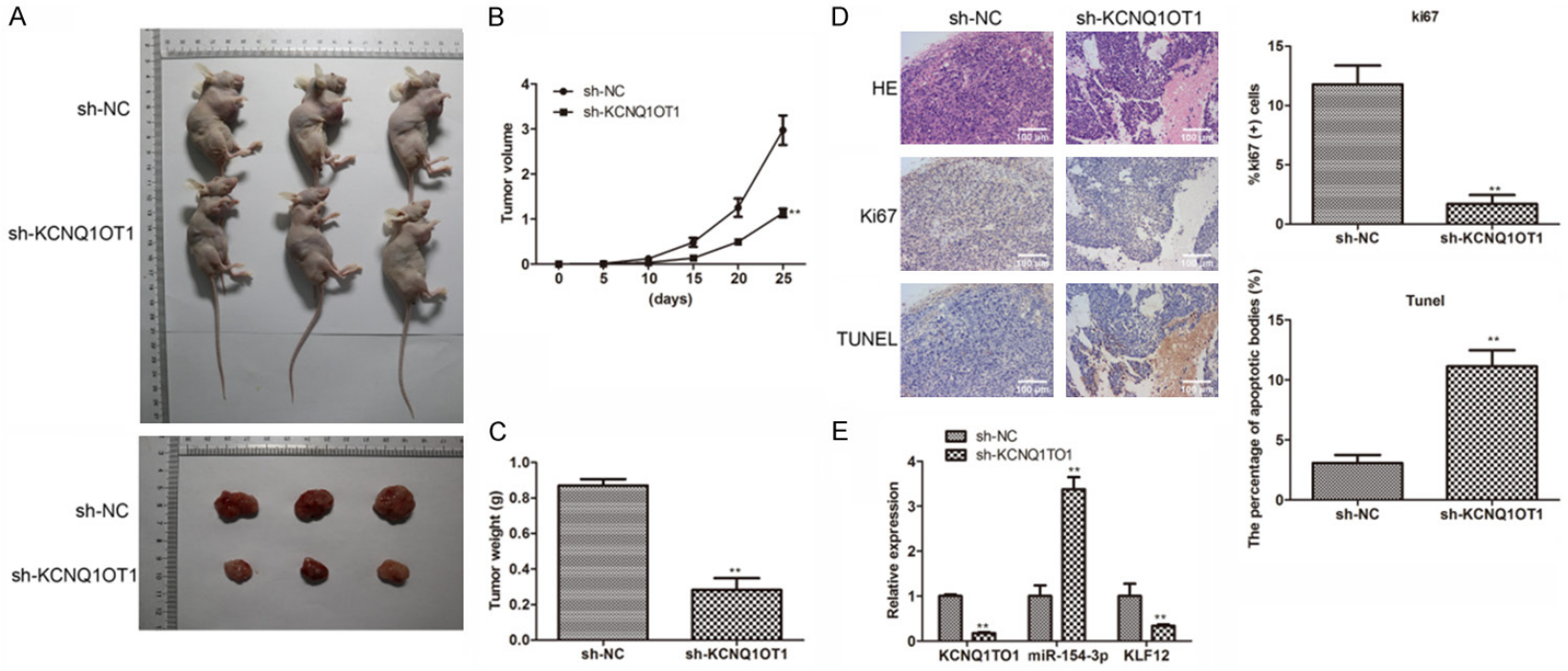

Figure 8. Downregulation of KCNQ1OT1 suppresses tumorigenesis of OS in vivo. Subcutaneous injected of KCNQ1OT1 stable knockdown U2OS cells. A: The tumor volume was measured when xenograft mice were sacrificed after 4 weeks; B: The tumor volume was measured every 5 days; C: The tumor weight was measured when xenograft mice were sacrificed; D: Histopathology was analyzed by HE staining and the percentage of Ki67-positive cells was measured by immunostaining in tumor tissues (200×); E: RNA levels of KCNQ1OT1, miR-154-3p and KLF12 in tumor tissues. Compared with control group, $^{**}P<0.01$. The number of nude mice was three in every group. Results represent the average of three independent experiments. OS: Osteosarcoma; KCNQ1OT1: KCNQ1 opposite strand/antisense transcript 1; NC: negative control.

resistance, epithelial-mesenchymal transition, cell cycle, and other cancer-related activities [17-19]. LncRNA is recognized to play a role in a range of malignancies, including breast cancer, lung cancer, colorectal cancer, and cervical cancer [20]. OS is a primary bone tumor that commonly occurs in children and adolescents [21]. A major and unsolved problem is the poor prognosis of transferred or relapsed OS patients [5]. As a result, a thorough understanding of the lncRNA mechanism may aid in the development of novel and successful therapy methods for OS patients.

Previous research has linked several lncRNAs to the development of OS. DLX6-AS1, for example, has been shown to improve OS stemness and Wnt signaling activation via miR-129-5p/DLK1 [22]. According to Fu et al., TTN-AS1 regulates OS growth and treatment resistance by competitively binding to miR-134-5p and stimulating the MBTD1 expression [23]. KCNQ1OT1 is an antisense transcript that affects the expression of several target genes and is found in the human KCNQ1 gene. In numerous types of cancer, cell proliferation, migration, and apoptosis have all been linked to KCNQ1OT1. KCNQ1OT1 expression increased and encouraged cell migration and epithelial-mesenchymal transition in colorectal cancer through the KCNQ1OT1/miR-217/ZEB1 feedback loop [24]. KCNQ1OT1 expression increased in NSCLC tissues, according to Dong et al., and elevated KCNQ1OT1 was linked to a poor prognosis. The oncogene KCNQ1OT1 boosted NSCLC tumor development via the miR-27b-3p/HSP90AA1 axis [25]. The involvement of KCNQ1OT1 in OS, on the other hand, has received minimal attention. Metastasis is the key to a poor prognosis in OS. The KCNQ1OT1 expression is increased in OS, and its knockdown decreased cell proliferation, migration, and invasion, and enhanced cell death. These findings are in line with earlier research [26].

LncRNAs are frequently functional as endogenous RNAs that compete with miRNA for binding, to exert their function. Hence, we speculated that KCNQ1OT1 affected OS process through sponging the specific miRNA. Through ENCORI, we predicted 508 miRNAs that binding to KCNQ1OT1. Subsequently, we selected 10 miRNAs reported as suppressor genes in the cancer process to detect their expression. MiR-154-3p was found to be the only gene that was downregulated in OS cells. MiR-154-3p has been identified as an autophagy-related non-coding RNA [27]. Furthermore, prior research found that miR-154-3p was considerably reduced in thyroid cancer and regulated cell proliferation and death by altering RHOA expression [28]. As a result, we speculated that miR-154-3p was involved in OS cell proliferation, migration, invasion, and death. In this study, KCNQ1OT1 promoted cell proliferation, migration, and invasion, and suppressed cell death by negatively influencing miR-154-3p expression.

MiRNAs impact gene translation in cancer by binding to its 3'UTRs region [29]. Based on the bioinformatics and RT-qPCR results, we found KLF12 expression was increased in OS cells. KLF12 has been reported in several cancers as a tumor suppressor gene [30, 31]. As a result, we hypothesized that the miR-154-3p/KLF12 axis influenced OS cell proliferation, migration, invasion, and death. We first confirmed that miR-154-3p inhibited KLF12 expression. Then, rescue experiments showed that downregulation of miR-154-3p could reverse the effects of KCNQ1OT1 deletion and this reversible effect was blocked by the knockdown of KLF12. The latest findings offer new perspectives on molecular treatment. Despite the fact that malignant tissues have higher KCNQ1OT1 expression than para-cancerous tissues, research into KCNQ1OT1 expression under miR-154-3p suppression was not possible due to time and technology constraints. The current study did not include any tests to demonstrate changes in cell proliferation, migration, or apoptosis as a result of KCNQ1OT1 overexpression. As a result, more research should be done in the future to corroborate the current findings. Finally, we revealed that KCNQ1OT1 was upregulated in OS tissues and cells, and this upregulation increased OS cell proliferation, migration, and invasion, and reduced cell death through the miR-154-3p/KLF12 axis (**Figure 9**).

In conclusion, KCNQ1OT1 is important for OS development, and that targeting KCNQ1OT1 could be a treatment approach for OS.

Disclosure of conflict of interest

None.

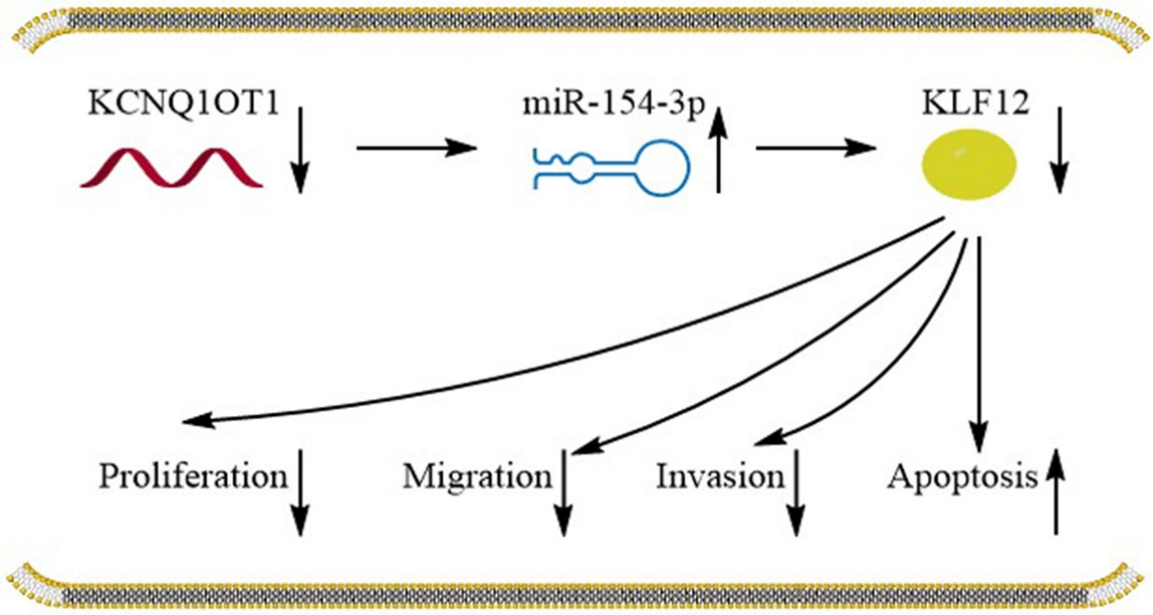

Figure 9. The schematic diagram of KCNQ1OT1 regulating miR-154-3p/KLF12 axis to promote the tumor progression in osteosarcoma. KCNQ1OT1: KCNQ1 opposite strand/antisense transcript 1.

Address correspondence to: Haitao Li, Department of Joint Surgery, Linyi People's Hospital, Intersection of Wuhan Road and Crouching Wohushan Road, Beicheng New District, Linyi 276000, Shandong Province, China. Tel: +86-0539-8012765; E-mail: hitolee19@sina.com

References

[1] Moore DD and Luu HH. Osteosarcoma. Cancer Treat Res 2014; 162: 65-92.

[2] Qian M, Gong HY, Yang XH, Zhao J, Yan WJ, Lou Y, Peng DY, Li ZX and Xiao JR. MicroRNA-493 inhibits the proliferation and invasion of osteosarcoma cells through directly targeting specificity protein 1. Oncol Lett 2018; 15: 8149-8156.

[3] Tang N, Song WX, Luo JY, Haydon RC and He TC. Osteosarcoma development and stem cell differentiation. Clin Orthop Relat Res 2008; 466: 2114-2130.

[4] Anderson ME. Update on survival in osteosarcoma. Orthop Clin North Am 2016; 47: 283-292.

[5] Harrison DJ, Geller DS, Gill JD, Lewis VO and Gorlick R. Current and future therapeutic approaches for osteosarcoma. Expert Rev Anticancer Ther 2018; 18: 39-50.

[6] Wang D, Song Z and Wang Z. Common mechanism of pathogenesis in various types of metastatic osteosarcoma. Oncol Lett 2017; 14: 6307-6313.

[7] Sasaki R, Osaki M and Okada F. MicroRNA-based diagnosis and treatment of metastatic human osteosarcoma. Cancers (Basel) 2019; 11: 553.

[8] Rossi M, Bucci G, Rizzotto D, Bordo D, Marzi MJ, Puppo M, Flinois A, Spadaro D, Citi S, Emionite L, Cilli M, Nicassio F, Inga A, Briata P and Gherzi R. Lncrna EPR controls epithelial proliferation by coordinating Cdkn1a transcription and Mrna decay response to TGF-beta. Nat Commun 2019; 10: 1969.

[9] Cui M, Chen M, Shen Z, Wang R, Fang X and Song B. LncRNA-UCA1 modulates progression of colon cancer through regulating the miR-28-5p/HOXB3 axis. J Cell Biochem 2019; [Epub ahead of print].

[10] Dong H, Hu J, Zou K, Ye M, Chen Y, Wu C, Chen X and Han M. Activation of LncRNA TINCR by H3K27 acetylation promotes trastuzumab resistance and epithelial-mesenchymal transition by targeting MicroRNA-125b in breast cancer. Mol Cancer 2019; 18: 3.

[11] Zhuang C, Ma Q, Zhuang C, Ye J, Zhang F and Gui Y. LncRNA GClnc1 promotes proliferation and invasion of bladder cancer through activation of MYC. FASEB J 2019; 33: 11045-11059.

[12] Paraskevopoulou MD and Hatzigeorgiou AG. Analyzing MiRNA-LncRNA interactions. Methods Mol Biol 2016; 1402: 271-286.

[13] Ye ZM, Yang S, Xia YP, Hu RT, Chen S, Li BW, Chen SL, Luo XY, Mao L, Li Y, Jin H, Qin C and Hu B. LncRNA MIAT Sponges miR-149-5p to

inhibit efferocytosis in advanced atherosclerosis through CD47 upregulation. Cell Death Dis 2019; 10: 138.
[14] Wang J, Zhang H, Situ J, Li M and Sun H. KCNQ1OT1 aggravates cell proliferation and migration in bladder cancer through modulating miR-145-5p/PCBP2 Axis. Cancer Cell Int 2019; 19: 325.
[15] Zhang S, Ma H, Zhang D, Xie S, Wang W, Li Q, Lin Z and Wang Y. LncRNA KCNQ1OT1 regulates proliferation and cisplatin resistance in tongue cancer via miR-211-5p mediated Ezrin/Fak/Src signaling. Cell Death Dis 2018; 9: 742.
[16] Li Y, Li C, Li D, Yang L, Jin J and Zhang B. LncRNA KCNQ1OT1 enhances the chemoresistance of oxaliplatin in colon cancer by targeting the miR-34a/ATG4B pathway. Onco Targets Ther 2019; 12: 2649-2660.
[17] Wu J, Chen H, Ye M, Wang B, Zhang Y, Sheng J, Meng T and Chen H. Long noncoding RNA HCP5 contributes to cisplatin resistance in human triple-negative breast cancer via regulation of PTEN expression. Biomed Pharmacother 2019; 115: 108869.
[18] Liu M, Zhang H, Li Y, Wang R, Li Y, Zhang H, Ren D, Liu H, Kang C and Chen J. HOTAIR, a long noncoding RNA, is a marker of abnormal cell cycle regulation in lung cancer. Cancer Sci 2018; 109: 2717-2733.
[19] Zhang Y, Li J, Jia S, Wang Y, Kang Y and Zhang W. Down-regulation of Lncrna-ATB inhibits epithelial-mesenchymal transition of breast cancer cells by increasing Mir-141-3p expression. Biochem Cell Biol 2019; 97: 193-200.
[20] Sanchez Calle A, Kawamura Y, Yamamoto Y, Takeshita F and Ochiya T. Emerging roles of long non-coding RNA in cancer. Cancer Sci 2018; 109: 2093-2100.
[21] Ritter J and Bielack SS. Osteosarcoma. Ann Oncol 2010; 21 Suppl 7: vii320-vii325.
[22] Zhang RM, Tang T, Yu HM and Yao XD. LncRNA DLX6-AS1/miR-129-5p/DLK1 axis aggravates stemness of osteosarcoma through Wnt signaling. Biochem Biophys Res Commun 2018; 507: 260-266.
[23] Fu D, Lu C, Qu X, Li P, Chen K, Shan L and Zhu X. LncRNA TTN-AS1 regulates osteosarcoma cell apoptosis and drug resistance via the miR-134-5p/MBTD1 axis. Aging (Albany NY) 2019; 11: 8374-8385.
[24] Bian Y, Gao G, Zhang Q, Qian H, Yu L, Yao N, Qian J, Liu B and Qian X. KCNQ1OT1/miR-217/ZEB1 feedback loop facilitates cell migration and epithelial-mesenchymal transition in colorectal cancer. Cancer Biol Ther 2019; 20: 886-896.
[25] Dong Z, Yang P, Qiu X, Liang S, Guan B, Yang H, Li F, Sun L, Liu H, Zou G and Zhao K. KCNQ1OT1 facilitates progression of non-small-cell lung carcinoma via modulating miRNA-27b-3p/HSP90AA1 axis. J Cell Physiol 2019; 234: 11304-11314.
[26] Shen Y, Xu J, Pan X, Zhang Y, Weng Y, Zhou D and He S. LncRNA KCNQ1OT1 sponges miR-34c-5p to promote osteosarcoma growth via ALDOA enhanced aerobic glycolysis. Cell Death Dis 2020; 11: 278.
[27] Wei DM, Jiang MT, Lin P, Yang H, Dang YW, Yu Q, Liao DY, Luo DZ and Chen G. Potential ceRNA networks involved in autophagy suppression of pancreatic cancer caused by chloroquine diphosphate: a study based on differentially-expressed circRNAs, lncRNAs, miRNAs and mRNAs. Int J Oncol 2019; 54: 600-626.
[28] Fan XD, Luo Y, Wang J and An N. miR-154-3p and miR-487-3p synergistically modulate RHOA signaling in the carcinogenesis of thyroid cancer. Biosci Rep 2020; 40: BSR2019-3158.
[29] Min A, Zhu C, Peng S, Rajthala S, Costea DE and Sapkota D. MicroRNAs as important players and biomarkers in oral carcinogenesis. Biomed Res Int 2015; 2015: 186904.
[30] Guo Y, Cao R, Zhang X, Huang L, Sun L, Zhao J, Ma J and Han C. Recent progress in rare oncogenic drivers and targeted therapy for non-small cell lung cancer. Onco Targets Ther 2019; 12: 10343-10360.
[31] Wang J, Pu J, Zhang Y, Yao T, Luo Z, Li W, Xu G, Liu J, Wei W and Deng Y. DANCR contributed to hepatocellular carcinoma malignancy via sponging miR-216a-5p and modulating KLF12. J Cell Physiol 2019; 234: 9408-9416.